Polyhedron 28 (2009) 2418–2430

Contents lists available at ScienceDirect

Polyhedron

journal homepage: www.elsevier.com/locate/poly

A study of nerve agent model organophosphonate binding with manganese-A_2B-corrole and -A_2B_2-porphyrin systems

Kibong Kim [a,b], Inkoo Kim [a], Nilkamal Maiti [a,b,1], Seong Jung Kwon [a], Daniela Bucella [c], Olga A. Egorova [a,b], Yoon Sup Lee [a], Juhyoun Kwak [a], David G. Churchill [a,b,*]

[a] Department of Chemistry and School of Molecular Science (BK 21), Korea Advanced Institute of Science and Technology (KAIST), 373-1 Guseong-dong, Yuseong-gu, Daejeon 305-701, Republic of Korea
[b] Molecular Logic Gate Laboratory, Korea Advanced Institute of Science and Technology (KAIST), 373-1 Guseong-dong, Yuseong-gu, Daejeon 305-701, Republic of Korea
[c] Department of Chemistry, Columbia University, 3000 Broadway, New York, New York 10027, USA

ARTICLE INFO

Article history:
Received 15 February 2009
Accepted 16 April 2009
Available online 24 April 2009

Keywords:
A_2B-corrole
trans-A_2B_2-porphyrin
Manganese
Organophosphonate
Nerve agent sensing
UV–Vis titrations
Cyclic voltammetry
Model nerve agent
Binding study

ABSTRACT

Herein the synthesis and binding studies of novel *trans*-A_2B-corrole and *trans*-A_2B_2-porphyrin derivatives are presented in comparing manganese(III)-organophosphonate (OP) binding (e.g., $M^{n+} \leftarrow O{=}PR(OR)_2$) capabilities. H_3(PFP-VC) [PFP-VC = 5,15-di(pentafluorophenyl)-10-(3-vinylphenyl)corrolate] was synthesized by way of literature procedures and was characterized by a variety of 2-D NMR spectroscopic techniques and single-crystal X-ray diffraction. These compounds represent the first example of 3-vinyl-phenyl-containing meso-substituted corroles or porphyrins. Mn(PFP-VC) (**3**) was treated separately with $(CH_3CH_2O)_2P{=}O(C_3H_6NMe_2)$, $(C_4H_9O)_2P{=}O(Me)$, $(C_2H_5O)_2P{=}O(CH_2COCH_3)$, $(CH_3CH_2O)_2P{=}O(Me)$, to give 1:1 adducts, as determined by UV–Vis spectroscopy (Job Plot), giving a *red* shift; $Ph_3P{=}O$, was also found to bind, but very weakly. The *trans*-A_2B_2-porphyrin analogue Mn(PFP-VP) (**4**) was also prepared by way of a literature procedure; related binding studies gave 1:1 organophosphonate-Mn(PFP-VP) adducts (Job Plot). A clean *blue* shift occurred for the Mn-porphyrins at higher organophosphonate loadings (K_a values: 6.7 (0.9)–11.9 (0.4) M^{-1}). DFT geometry optimizations of $O{=}P(OMe)_2Me$ binding and formal Mn–O or P–O cleavage products in the unsubstituted *neutral* Mn-corrolato and -porphyrinato systems with a range of metal-based spin states revealed greatest stability in formal phosphoryl oxygen binding (energies: 11–13 kcal/mol) for the Mn-corrole (*singlet*); the Mn-porphyrin (*sextet*) was also quite stable.
© 2009 Elsevier Ltd. All rights reserved.

1. Introduction

Macrocyclic polypyrroles are motifs of great ubiquity, constituting a range of both synthetic metal complexes and natural systems (i.e., hemoglobin, corrin and chlorophylls) (Fig. 1). Of note, the porphyrin sub-class is crucial in oxygen-atom transfer [1], and in analyte binding (e.g., O_2), with the ability to host a variety of Lewis bases in forming important adducts in biology. Corroles, members of a currently greatly expanding class of contracted porphyrin, are gaining greater visibility through the sub-field's major contributors: Gross [2], Gryko [3,4], Kadish [5,6], and Paolesse [7]. Corroles differ from porphyrins in two important ways: they possess one direct pyrrole–pyrrole bond in place of one methine (C–H) linkage, and they are *tri*valent instead of divalent. This difference allows for metal-corrolato species to possess a likeness to Nature's hemes through their aromaticity on one hand, and a corrin-like structural cavity that bears a *tri*valent cavity instead of a monovalent core (Fig. 1) on the other hand. These features enable a stabilization of transition metal ions in valence states [8] that are systematically higher than those known in the respective porphyrins.

Through the study of transition metal coordination chemistry, adequate control of complex color, electronics, sterics, and molecular geometry can, in theory, be imparted, especially through the use of a rigid delocalized ligand corrole or porphyrin frame. A delocalized and rigid frame may also be fluorogenic. Mn-corrolato species, however, do not appear to be promising in this respect. Thus, to determine whether a porphyrin or corrole framework, or both, is of utility in the optical or otherwise sensing of organophosphonate is the goal of these solution studies. Since our primary focus here is on nerve agent model [O=P] oxygen metal ion binding, we also undertook theoretical calculations to fully determine M-corrole $O{=}P(OR)_2R$ binding energies using model systems. Understanding the features and substitutions that enhance, or detract from, the binding capabilities of metalloporphyrin derivatives are essential in the rational development of these systems as detection platforms in hazardous analyte sensing. Generally, metallocorroles

* Corresponding author.
E-mail address: dchurchill@kaist.ac.kr (D.G. Churchill).
[1] Present address: Midnapore College, Midnapore, Paschim Medinipur, West Bengal 721101, India. Tel.: +82 42 350 2845; fax: +82 42 350 2810.

0277-5387/$ - see front matter © 2009 Elsevier Ltd. All rights reserved.
doi:10.1016/j.poly.2009.04.020

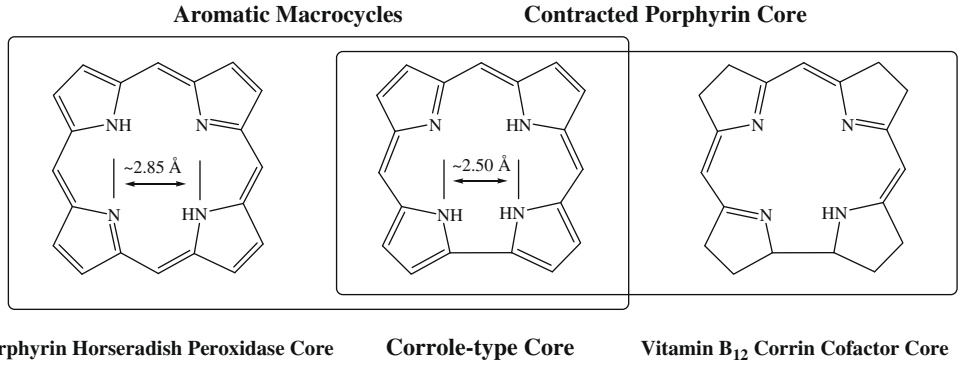

Fig. 1. A comparison of the macrocyclic porphyrin, corrole and corrin (vitamin B_{12} cofactor) frames. Note: the left and middle structures are the basis of geometry optimization calculations, illustrated below in Figs. 11 and 12.

and metalloporphyrins show some promise as selective analyte sensing platforms. Corroles have been explored as CO sensors of sufficient selectivity when testing with competitive analytes such as O_2 and N_2. The nature of the metal (e.g., Co^{3+}) as well as corrole substitution play essential parts in the Lewis acidity of the metal center [9], which is the sensing core. Metallocorroles also have good reproducibility and stability over a term of months as "electronic noses." In a related report, there was no loss of corrole "monomer" from a thin layer array over a four-week period of continual use [10]. Precedent for related metallo*porphyrin*-based sensors comes from reports by Di Natale and coworkers [11–13]. Porphyrin derivatives have also been the subject of computational efforts in the context of analyte selectivity [14–17].

The types of analytes we chose to study here are organophosphonates, relatives of the extremely deadly organophosphonate nerve agents (Fig. 2). While there have been significant efforts to fully decontaminate all stockpiles, undertaken in good faith to abide by the time-table set forth by the Chemical Weapons Convention (CWC), there are still significant amounts of organophosphonate-based chemical weapons in North America as well as in Eurasia that, to date await complete destruction and remediation. This impetus, along with potential terrorist agent development and use, support the need for continued investigations into improved real-time sensing devices [17].

Cyclic polypyrrole ligand-based sensing platforms may be able to efficiently and selectively mediate in techniques such as piezoelectric crystal sorption detection which are the centerpiece of portable and growingly reliable nerve agent detection/discernment. The possibility of metallocorroles serving in nerve agent detection and decontamination is suggestive from results reported by Gross and coworkers in which $Ph_3P{=}O$ forms an adduct with Mn(III)tpfcorrolato; this adduct can also be formed from the manganyl [Mn=O] species upon addition of PPh_3 [18]. The crystal structure in which triphenylphosphine oxide is coordinated to tris-pfp-Mn-corrole [19a,19b] can be compared to one in which there exists a free Mn(III)corrolato center [19c].

Mn-corrole-based organophosphonate nerve agent sensing can be explored in a variety of ways. Our approach involved preparing closely related Mn-corrolates that bear stability imparted from the pentafluorophenyl groups but that also contain a 10-position *meso*-aryl group that contains an attachment point. We were able to develop the corrole and the related porphyrin system for comparison. We also go further here theoretically, in determining how oxygen binding of organophosphonate nerve agent mimics, and how the phosphoryl oxygen can formally migrate from the Mn=O group; this can be treated theoretically (*vide infra*). While organophosphonates have different electronic and steric properties as the simpler $Ph_3P{=}O$ molecule [19], we can look at a variety of organophosphonate species: $(CH_3CH_2O)_2P{=}O(C_3H_6NMe_2)$, $(C_4H_9O)_2P{=}O(Me)$, $(C_2H_5O)_2P{=}O(CH_2COCH_3)$, $(CH_3CH_2O)_2P{=}O(Me)$, $Ph_3P{=}O$ (Fig. 2), and other analytes with compounds **3** or **4** (Scheme 1) [20].

In terms of the preparative chemistry of corroles, extremely practical pathways to A_2B-corroles have been reported by Gryko and coworkers [3,4]. Thus, we have prepared *meso*-thienyl-A_2B-corroles species with the well-known C_6F_5-substitution, and also the 3-vinylphenyl substitution which may facilitate chemisorption *via* sulfhydryl groups of functionalized surfaces [21]. We have also prepared the analogous porphyrin system to compare analyte binding in two closely related systems.

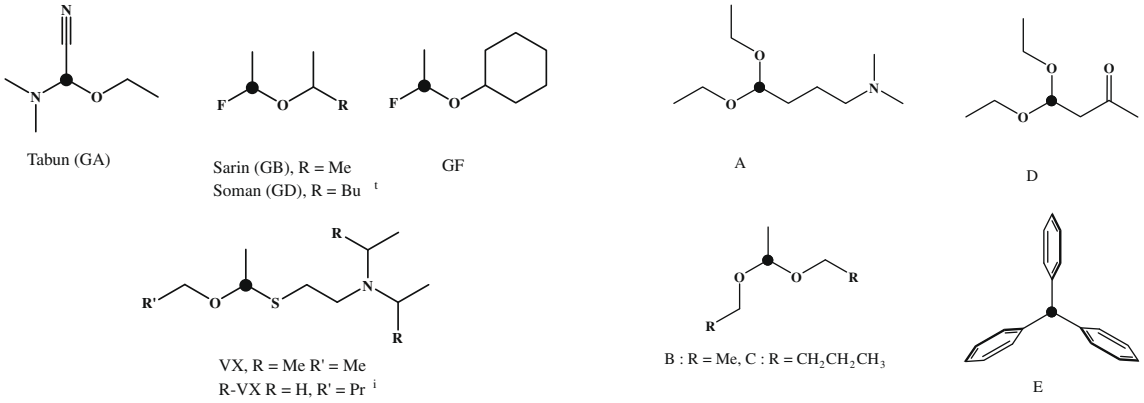

Fig. 2. ● = [O=P] group. (*left*) Common organophosphate nerve agents. G- and V-type chemical warefare (nerve) agents. (*right*) Phosphorus-containing molecules used in this study.

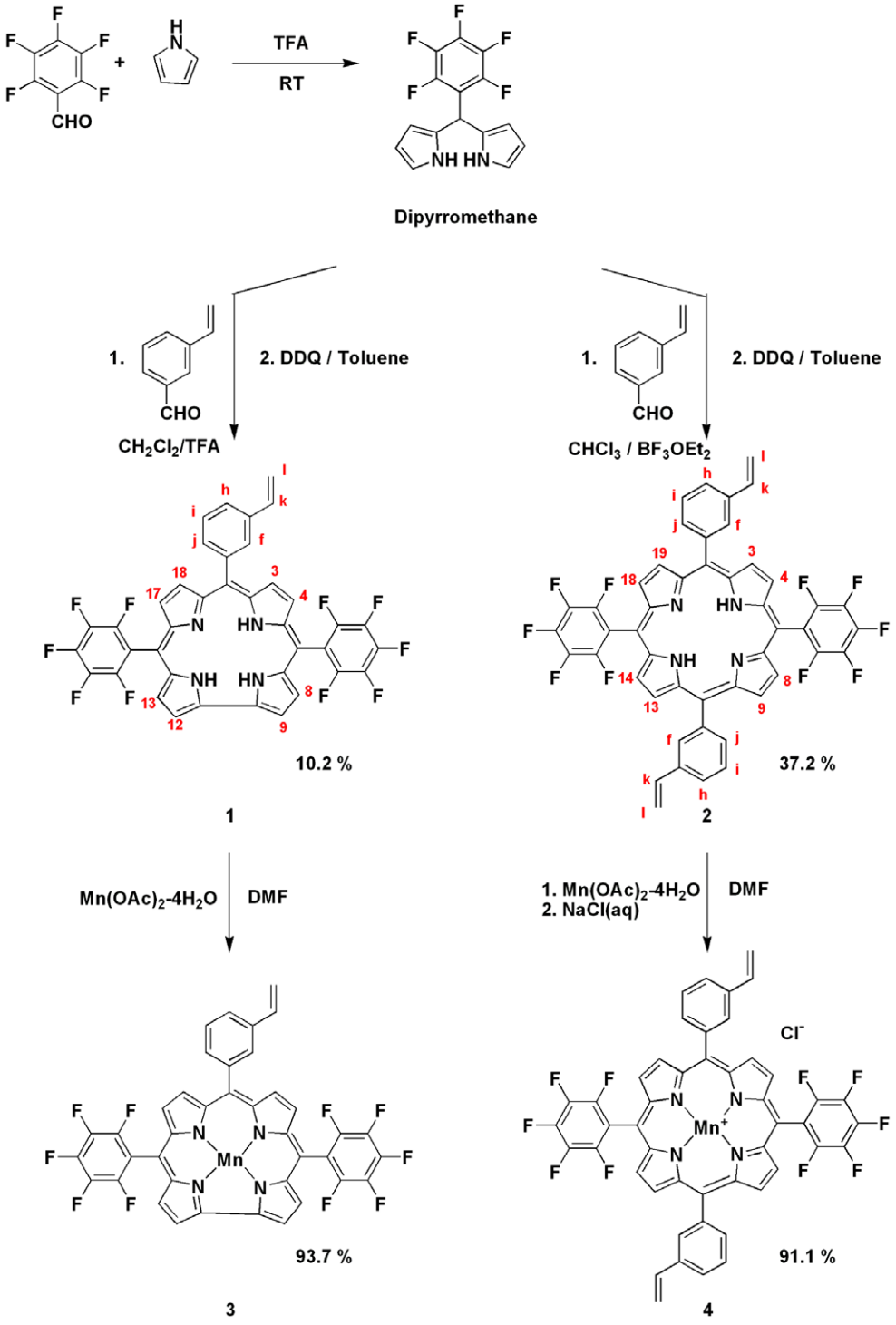

Scheme 1. The synthesis of corroles and porphyrins and their products of metallation reported herein. Percent yields are included next to each molecule. The crystallographic report of **1** appears below.

2. Results and discussion

2.1. Synthesis and characterization

Corrole preparation began with the generation of dipyrromethane prepared by the literature method of Lindsey and coworkers [22] involving the condensation of pyrrole and aldehyde. The synthesis of A_2B corroles were adapted from well-known literature reports [23,4], which begins with the dipyrromethane and involves the addition of benzaldehyde derivative followed by oxidation, usually effected by DDQ. We have previously reported 2- and 3-thienyl-dipyrromethanes [24a] as well as meso-substituted A_3-corroles that were prepared analogously as reported previously in *Polyhedron* [24b]. While the A_2B_2 porphyrin (Compound **2**) can sometimes be satisfactorily isolated as a by-product in the corrole-generating reaction above [25a], this species was prepared using more optimal conditions in accordance with a previously reported literature method [25b] to give a microcrystalline sample of

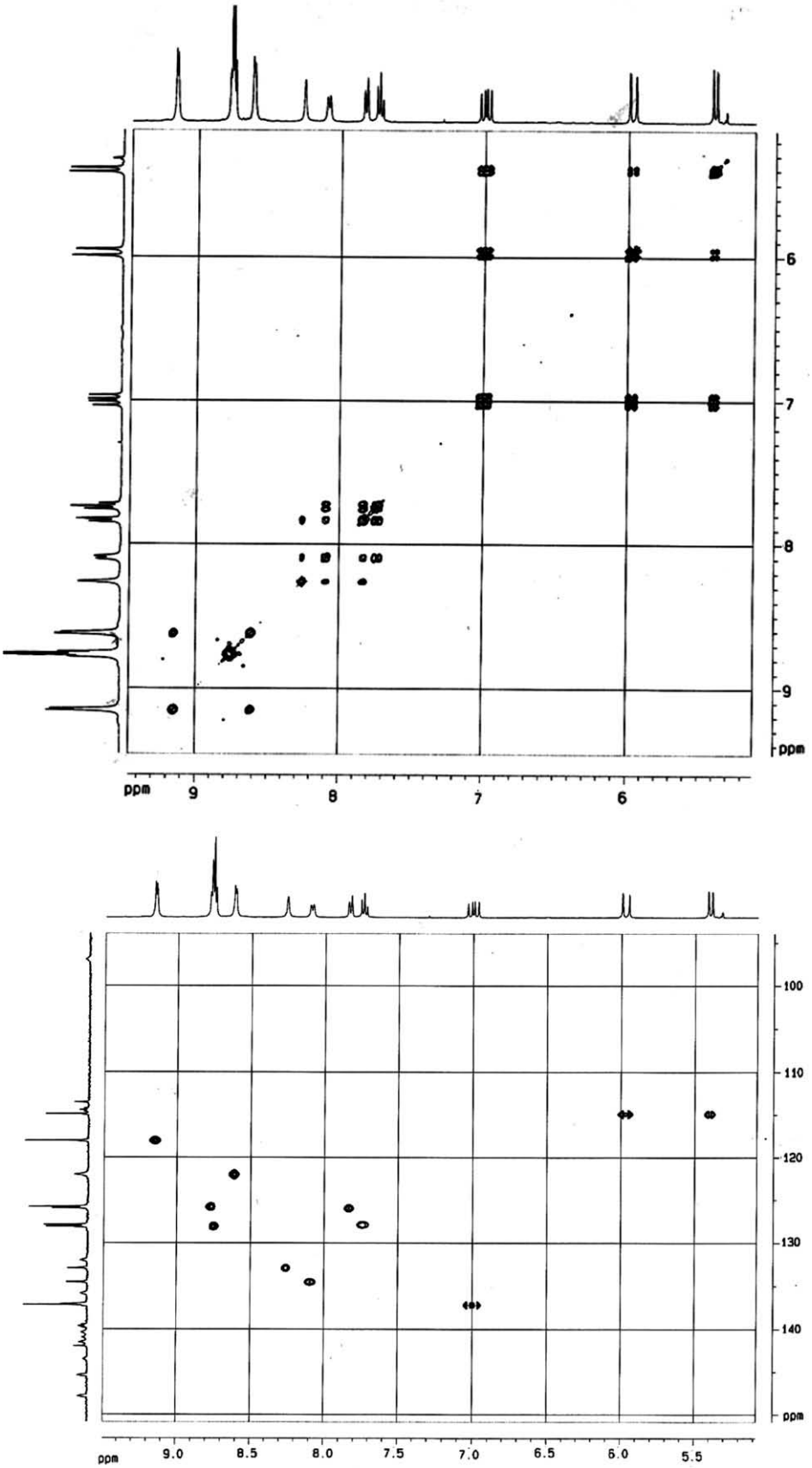

Fig. 3. (*top*) The aromatic portion of the ^{1}H–^{1}H COSY NMR spectrum showing all C–H protons, and (*bottom*) ^{1}H–^{13}C HMQC NMR spectrum showing all carbon resonances, for H_3(PFP-VC).

the species formulated as the Mn(III)porphyrinato chloride (**4**) [25c]. Thus, a solid of compound **2** was obtained through recrystallization in 37% yield (See Section 4). Suitability of this as an oxygen-atom transfer catalyst has been previously reported [20b,20d].

Characterization of the new compounds **1**–**4** reported herein was made mainly by spectroscopic techniques: ^{1}H NMR, ^{13}C NMR and UV–Vis spectroscopic studies (e.g., Fig. 3 and Supporting Information) as well as CV measurements. We also relied on 2-D NMR spectra, which are used conveniently because of the fully unsaturated nature of Compounds **1** and **2** which have resonances gathered in the aromatic region (5–9 ppm). The substitution (as in Compound **2**) as well as other corrole features give rise to clearly assignable cross-peaks in 2-D NMR spectra such as the ^{1}H–^{1}H COSY and ^{1}H–^{13}C HMQC NMR spectra of H_3(PFP-VC) provided in Fig. 3. For mass spectrometry, the presence of the expected species comes from the inspection of isotopic clusters centered at calculated values for complexes **1**–**4** (Supporting Information). Additional characterization is provided by single-crystal X-ray diffraction for compound **1**, presented below.

2.2. UV–Vis spectroscopic detection of organophosphonate via titrations in CH_2Cl_2

While fluorescence characteristics of corroles can be intense and unique, incorporation of Mn^{3+} renders the complexes non-fluorescent. Thus, herein we rely on UV–Vis absorption spectroscopic changes. Electronic absorption spectra of Mn(PFP-VC) (**3**) and Mn(PFP-VP) (**4**) with different organophosphonate species bearing various binding atoms will be presented in this section. Detailed titrimetric spectra are provided in Figs. 4–6 for Mn corroles and Figs. 7 and 8 for Mn-porphyrins. These trials all show a diminution in the Soret band at 411 nm when Compound **3** is used. A new band at 473–483 nm grows in as indicated by a label in each figure. Triphenyl phosphine was also tested as an analyte; it also has the capacity to bind through its (lone) oxygen atom, and, along with the sterics and rigidity of the phenyl groups, does so less efficiently, as shown by comparatively smaller changes in the spectrum (Supporting Information). This is surprising in light of the fact that a crystal structure of a closely related adduct is known. It is interesting to note that other, possibly better binding, phosphorus oxide species were *not* studied as of yet in this context.

A determination of ligand-to-metal complex stoichiometry in this reaction mixture was performed by the method of continuous variation. Titrimetric trials for A–D (Fig. 2) were performed, as shown e.g., in Fig. 4, in which a portion of Mn(PFP-VC) in dichloromethane was titrated by $(CH_3CH_2O)_2P{=}O(C_3H_6NMe_2)$ (**A**). Clear growth of new bands appear at 473 and 634 nm. The $(CH_3CH_2O)_2P{=}O(C_3H_6NMe_2)$ species is interesting in that there is a pendant amino group in virtually the same place as that seen for VX (Fig. 2), relative to the central phosphorus [26,27]. The next titration involved $(C_2H_5O)_2P{=}O(CH_2COCH_3)$ which afforded new bands in the electronic absorption spectra at 483 and 631 nm. The $(CH_3CH_2O)_2P{=}O(Me)$ species gave bands at 481 and 635 nm. Finally, $(C_4H_9O)_2P{=}O(Me)$ gave bands at 481 and 631 nm (Supporting Information). For these four species (Figs. 4–6, and S14) the Job plots involving the method of continuous variation were prepared; in all these cases (Insets of Figs. 4–6, and S14), the maximum peak at a mole fraction of ~0.5 is indicative that the solution stoichiometry is the expected 1:1 ligand-to-metal binding ratio. This is in accordance with the notion that the organophosphonate species will bind mainly through the phosphoryl [O=P] oxygen atom. The possibility of its binding through other heteroatoms, albeit more weakly, will not be considered herein.

There may be some concern that the Mn corrolato system valence state may change during, or prior to, analyte binding in light of (i) Mn^{4+} being an air stable metallocorrolate oxidation state and (ii) the involvement of stabilizing axial ligation [25e]. Importantly, to support our formulated Mn valence states, EPR spectroscopy for the $Ph_3P{=}O$ adduct of the Mn(tpf)corrolato species reported by Gross et al., reveals a Mn(III) ($S = 2$) metal center [19a]. This characterization excludes the possibility for the Mn(II) "radical cation" species [25d] and also for a Mn(IV) center. Compound **3** differs from the Mn(tpf)corrolato species only by the 10-position aryl group in which a 3-vinyl phenyl group replaces a pentafluorophenyl group. This small substitution will unlikely change the chemistry dramatically. Further experimental support that we do *not*

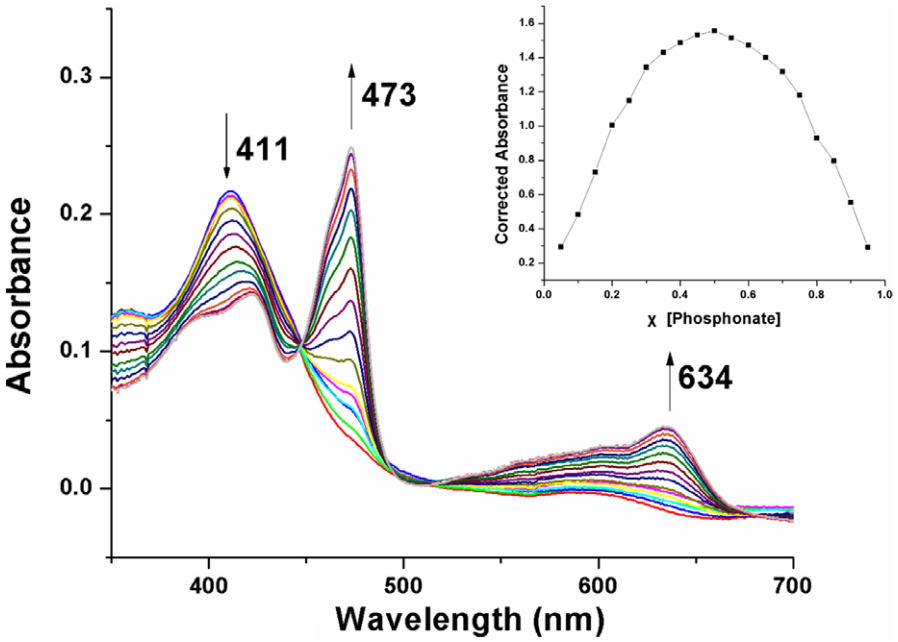

Fig. 4. Electronic absorption spectra of Mn(PFP-VC) [4.69×10^{-6} M] treated in dichloromethane with $(CH_3CH_2O)_2P{=}O(C_3H_6NMe_2)$ [5.06×10^{-3} M] (10–50 (by 10), 100–650 (by 50) μL). Inset: Job Plot for a (binary) mixture of **3** with $(CH_3CH_2O)_2P{=}O(C_3H_6NMe_2)$ showing a 1:1 stoichiometric correspondence.

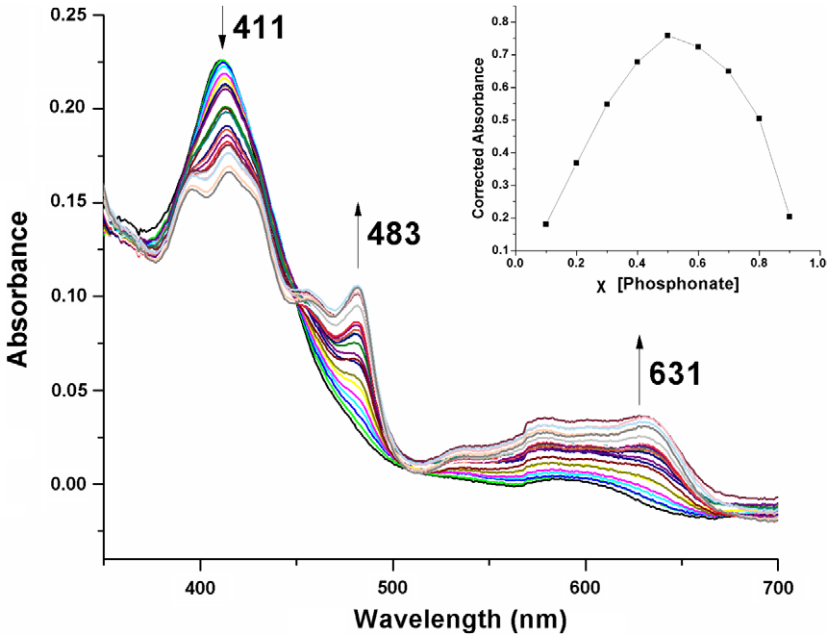

Fig. 5. Electronic absorption spectra of Mn(PFP-VC) [4.69×10^{-6} M] in the presence of various amounts (50–1100 (by 50) μL) of $(C_2H_5O)_2P{=}O(CH_2COCH_3)$ [1.51 M] in dichloromethane. Inset: Job plot for a binary mixture of **3** with $(C_2H_5O)_2P{=}O(CH_2COCH_3)$.

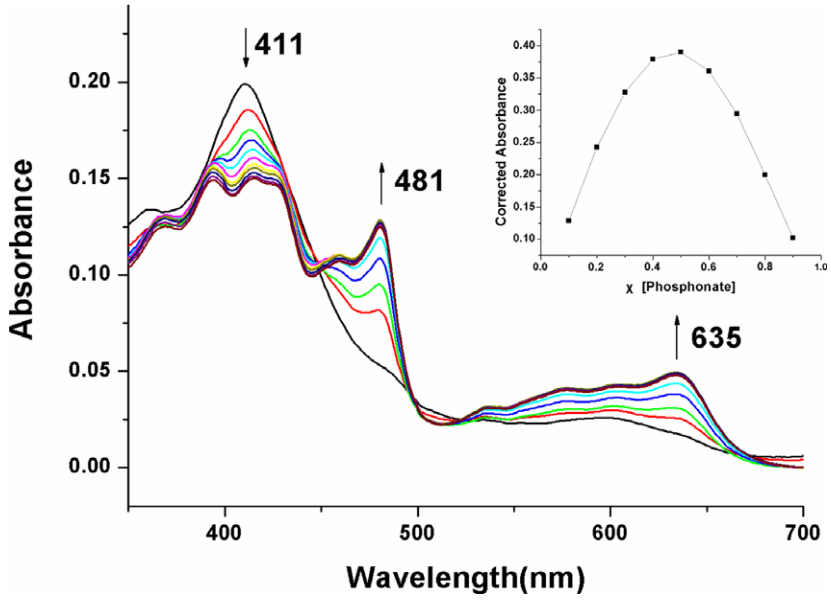

Fig. 6. Electronic absorption spectra of Mn(PFP-VC) [4.69×10^{-6} M] in the presence of various amounts (50–500 (by 50) μL) of $(CH_3CH_2O)_2P{=}O(Me)$ [2.74 M] in dichloromethane. Inset: Job Plot for a binary mixture of **3** with $(CH_3CH_2O)_2P{=}O(Me)$.

access *reduced* Mn-corrolato forms comes from the fact that electro-reduced forms of Mn(III) are unstable towards solvents, i.e., methylene chloride [25e], especially in the absence of a clear reductant. Additional support for Mn(III)corrolato ones comes from an analogous corrolazine compound reported by Goldberg and coworkers in which a shoulder at 722 nm in the UV–Vis spectrum is assigned to the Mn(III)O=PPh_3 adduct [19b]. In terms of Mn-corrole coordination, the Mn(III) species may exist in solution with one more axial MeCN. To further delve into the particulars of the valence state as well as a consideration of substrate/anion binding, we can turn to electrochemical studies discussed below that introduces a detailed report by Kadish and coworkers [25f] who have addressed how to best assign the valence state of the metal ion under various conditions [8].

We also studied the related binding for the *porphyrin* compound Mn(PFP-VP) with $(C_4H_9O)_2P{=}O(Me)$, $(C_2H_5O)_2P{=}O(CH_2COCH_3)$, and $(CH_3CH_2O)_2P{=}O(Me)$. These analytes were used in UV–Vis titrimetric trials whose results are plotted in Figs. 7 and 8 (and Supporting Information). All four assays give rise to clear changes compared to those of the Mn-corrole cases in that the Soret band undergoes moderate diminution and blue shifting only to give a new band in the range of 450–460 nm. While there is a clean spectral change, a much greater amount of analyte was required to effect this optical change than was needed in the corrole case, thus,

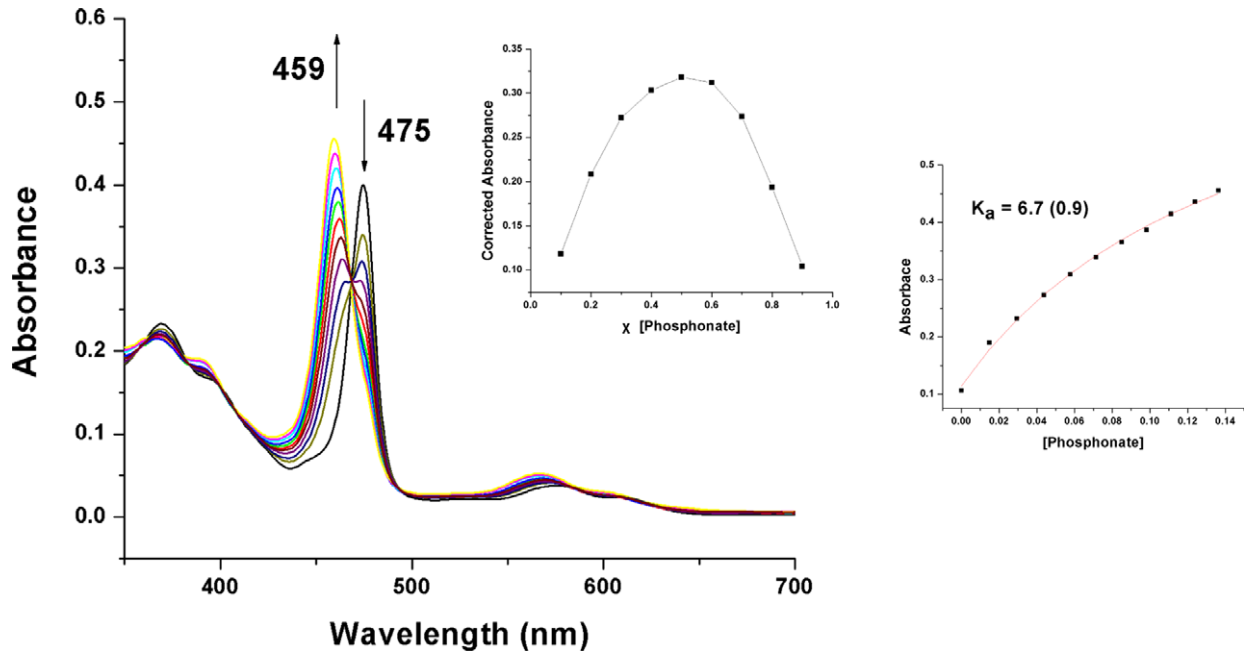

Fig. 7. Electronic absorption spectra of Mn(PFP-VP) [5.00×10^{-6} M] in dichloromethane upon titration with various amounts of $(C_2H_5O)_2P{=}O(CH_2COCH_3)$ [1.50 M] (20–200 (by 20) μL). Inset: Job Plot for a binary mixture of **4** with $(C_2H_5O)_2P{=}O(CH_2COCH_3)$.

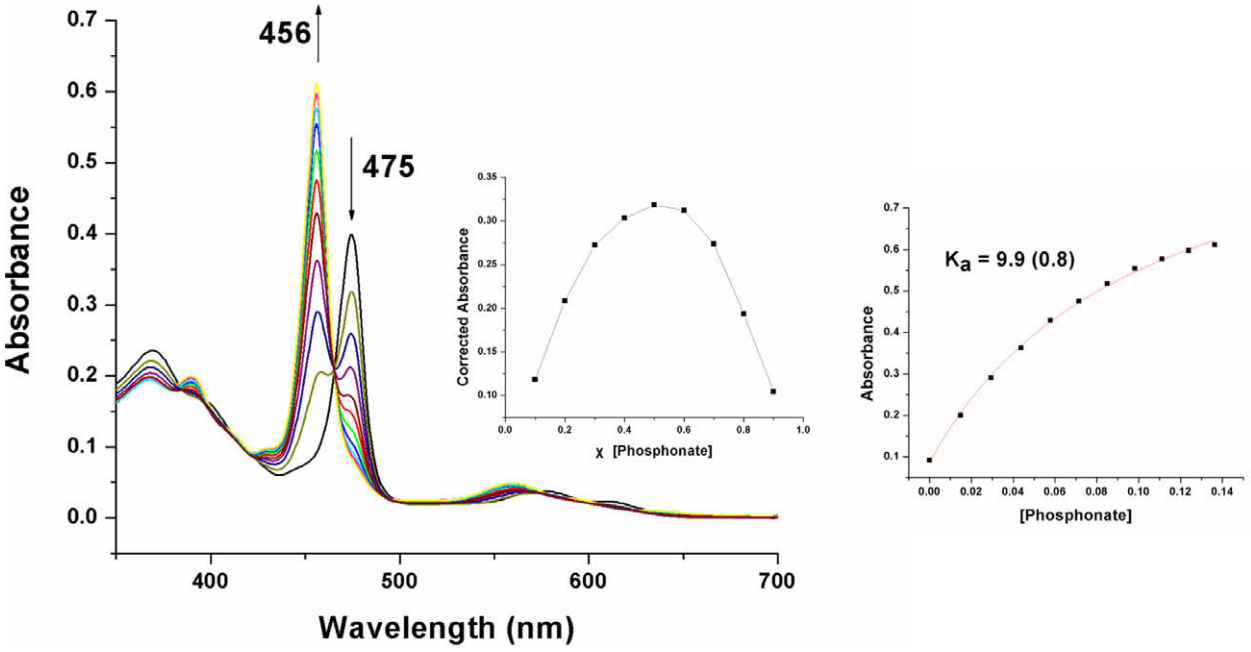

Fig. 8. Electronic absorption spectra of Mn(PFP-VP) [5.00×10^{-6} M] in dichloromethane in the presence of various amounts of $(C_2H_5O)_2P{=}O(Me)$ [1.50 M] (20–200 (by 20) μL). Inset: Job Plot for a binary mixture of **4** with $(C_2H_5O)_2P{=}O(Me)$.

these porphyrin-based systems are obviously less sensitive and less impressive as a potential sensing platform in the context of organophosphonates. This is in line with the tendency for a more in-plane metal ion in which a larger deviation from the [N_4] plane may encourage stronger analyte binding. The binding constants (K_a) values were measured by way of an equation reported by Valeur et al. [32] and are provided below as insets (Figs. 7 and 8). The binding constant for $(C_2H_5O)_2P{=}O(CH_2COCH_3)$ is 6.7 (0.9) M^{-1}; that for $(C_2H_5O)_2P{=}O(Me)$ is 9.9 (0.8) M^{-1}; and, that for $(C_4H_9O)_2P{=}O(Me)$ is 11.9 (0.4) M^{-1}.

As in the corrole case, we believe that this porphyrin system maintains an unchanged valence state upon binding. We should note, however, that a similarity in blue shifting pattern occurs for Mn=O formation. The oxo-Mn-(*meso*-tetrakis-2,3,5,6,-tetrafluoro-*N*,*N*,*N*-trimethyl-4-aniliniumyl)porphyrinato species (427 nm) gives a band at for the Mn(III)-porphyrinato at ~450 nm, upon

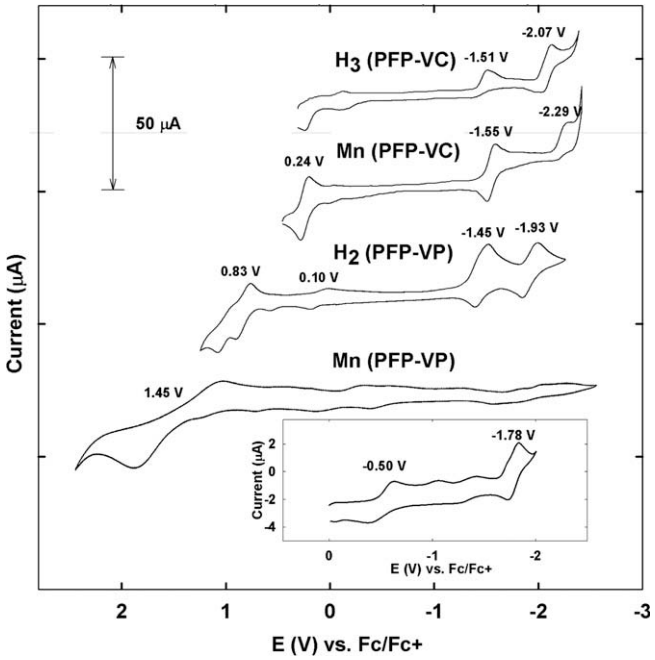

Fig. 9. Cyclic voltammetry data for compounds **1–4**, [3.0 mM], respectively, at room temperature in benzonitrile. Refer to Section 4 for further details. Half-wave potentials and peak potentials for **1–4** in benzonitrile. The inset is from a measurement of compound **4** at 1.0 mM.

carbamazepine epoxidation (10,11-position oxidation) [25c]. Thus further determinations for our porphyrin species will need to be made through future work.

2.3. Cyclic voltammetry (CV)

Electrochemistry often enables for the useful assignment of metal and ligand oxidations and affords a look at an analysis of the state of the M^{n+} of the metal complex, especially when considering transition metal ions such as manganese. A variety of recent reports of Mn-corrolates are available [25f]. The cyclic voltammograms have been obtained for compounds **1–4** and are provided below in Fig. 9. The cyclic voltammograms which include half-wave potentials/peak potentials (versus Ag/Ag^+ or Fc/Fc^+ or SCE) were obtained in PhCN. As revealed by the CV curve in Fig. 9, the reduction potentials for **3** are −1.55 and −2.29 V (versus SCE). This value is very similar to the reduction potentials of −1.51 and −2.07 V (versus SCE) for the metal free corrole **1** and has been assigned as corrole-centered reductions. The oxidation potential for **3** (0.24 V versus SCE) is assigned to the metal center, and is less than that for the Mn(tpf)corrole (0.71 V versus SCE), indicating **3** is more easily oxidized than the Mn(tpf)corrole [28]. A comparison to Mn(Mes_2Ph)corrole can also be made (Table 1). This species has been studied in considerable detail and has a variety of reduction and oxidation potentials depending on the solvent and axial anion coordination which are similar when in non aqueous media [25f].

Data was also obtained for the porphyrin-based species **2** and **4** (Scheme 1). For the free-base porphyrin, the first reduction occurs at −1.45, and −1.93 V, and the oxidization values occur at 0.10 and 0.83 V. For the Mn(III)-porphyrin chloride species, the first small $E_{1/2}$ reduction occurs at −0.50 with another occurring out at −1.78 V (Inset, Fig. 9); a broad $E_{1/2}$ of oxidation exists at 1.45 V.

2.4. Structural characterization of compound *1*

We also provide herein the crystal structure of 5,15-bis(pentafluorophenyl)-10-(3-vinylphenyl)corrole (**1**) (Fig. 10). The molecular structure of **1** confirms the presence of the vinyl moiety found also naturally in hemes; it points down and is suggestive of a clear surface anchoring group [21]. This serves as the first structural example of molecule with a 3-vinyl-phenyl dipyrrin/dipyrromethane fragment. There exists a plausible hydrogen bonding network between pairs of molecules as well (Supporting Information). Crystallographic packing structures provided for this structural solution separately along all three axes have been prepared (Supporting Information).

2.5. DFT calculations on bare corrole and porphyrin model systems

To try to understand the differences between neutral [28b] Mn–corrole and Mn–porphyrin organophosphonate binding and related transformations, we undertook DFT calculations using an unsubstituted corrole or porphyrin, oxygen atom, and the requiste phospho*nate*/*-ite* fragments. While calculations have previously been undertaken in trying to understand porphyrin M=O species, the details of M–O–P interactions are particularly informative in the present context. Electronic energies and geometries for formal M–O and P–O bond cleavage products for various metal-based spin states are illustrated in Figs. 11 and 12. The spin states in the corrole case were the singlet, triplet and quintet. Going from the bench-mark "Compound I"-like metal oxo species [1,29] the differences in energies in the middle section and those on the left represent the energy of formal O–M cleavage, whereupon the O-atom formally migrates from the metal to the phosphorus atom of the phospon*ite* ($POMe_2Me$). Going from the middle set to the right side set (in Fig. 11) formally signifies the attachment of the phosphine atom to the manganyl O-atom. This atom then becomes engaged as the donor atom in a Lewis base adduct with the metal center. The presence of the O=P bond, as well as a favorable dative interaction of ~10 kcal/mol gives this species (for the singlet) the lowest energy state. How the O-atom rearranges from an $X_2(L)$ donor to an L-type donor is a very interesting point for later consideration. A similar profile exists for the neutral Mn-porphyrinato and its derivatives (Fig. 12). Herein, the doublet, quartet, and sextet spin states were calculated. A much higher energy profile for the

Table 1
A comparison of reduction and oxidation potentials of **3** and related compounds Mn(Mes_2Ph)-corrole and Mn(tpf)corrole in various solvents.

	Solvent	3rd ox. (V)	2nd ox. (V)	1st ox. (V)	1st red. (V)
Mn(Mes_2Ph-Corrole) [25f]	CH_2Cl_2	–	1.00	0.32 (0.03)[b]	–
Mn(Mes_2Ph-Corrole) [25f]	PhCN	1.83[a]	1.07	0.45 (0.12)[b]	−1.36, −1.64
Mn(Mes_2Ph-Corrole) [25f]	Pyridine	–	–	0.42	−1.46
Mn(tpf)Corrole [28]	CH_2Cl_2	–	–	0.71	–
Compound **3** [*this article*]	PhCN	–	–	0.24	−1.55, −2.29

All values referenced to the SCE except for **3** which was reported versus the ferrocene/ferrocenium ion redox couple.; SCE = (Fc/Fc^+) + 0.40 V; $(Fc/Fc^+) = (Ag/Ag^+) - 0.092$ V; $E_{1/2}$ TBAP = tetrabutylammonium perchlorate.

[a] Scan rate 0.1 V/s.

[b] Extra peaks are due to the varation of axial ligation. A dash indicates an unreported or unobtainable value.

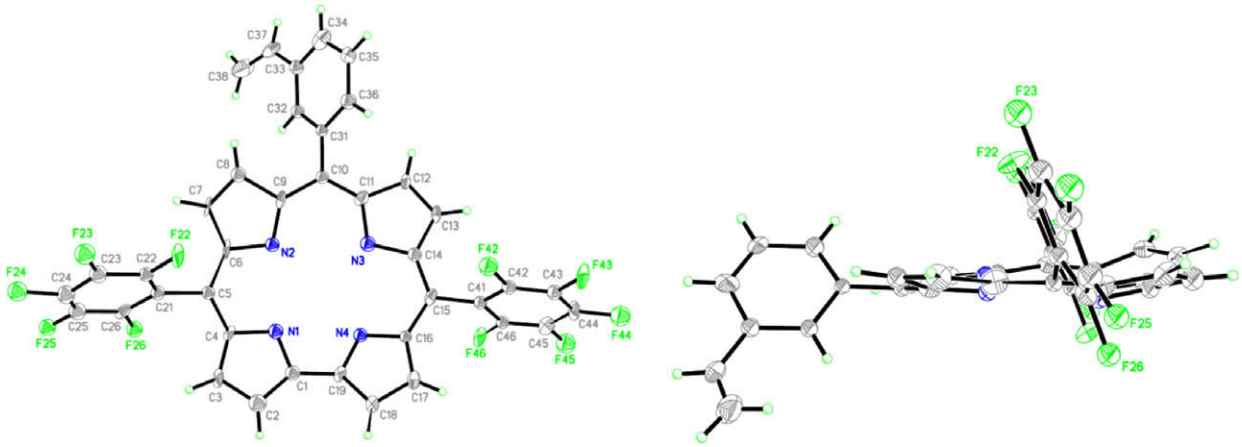

Fig. 10. Top and side views of **1** (CCDC 684999). Hydrogens are retained for clarity. X-ray diffraction study parameters: chemical formula $C_{39}H_{18}F_{10}N_4$, fw 732.14, Space group $P\bar{1}$, a = 10.077(13) Å, b = 13.359(18) Å, c = 14.907(19) Å, α = 113.113 (17)°, β = 90.83(3)°, γ = 105.165(17)°, V = 1766(4) Å^3, Z = 4, μ = 0.121 (mm^{-1}), R_1 = 0.2094, wR_2 = 0.4016 {$R_1 = (\Sigma||F_o| - |F_c||)/\Sigma|F_o|$; $wR_2 = [(\Sigma(F_o^2 - F_c^2)^2)/\Sigma w(F_o^2)^2]^{1/2}$}, ρ_{calcd} = 1.404 (mg/m^3), Temp = 243(2).

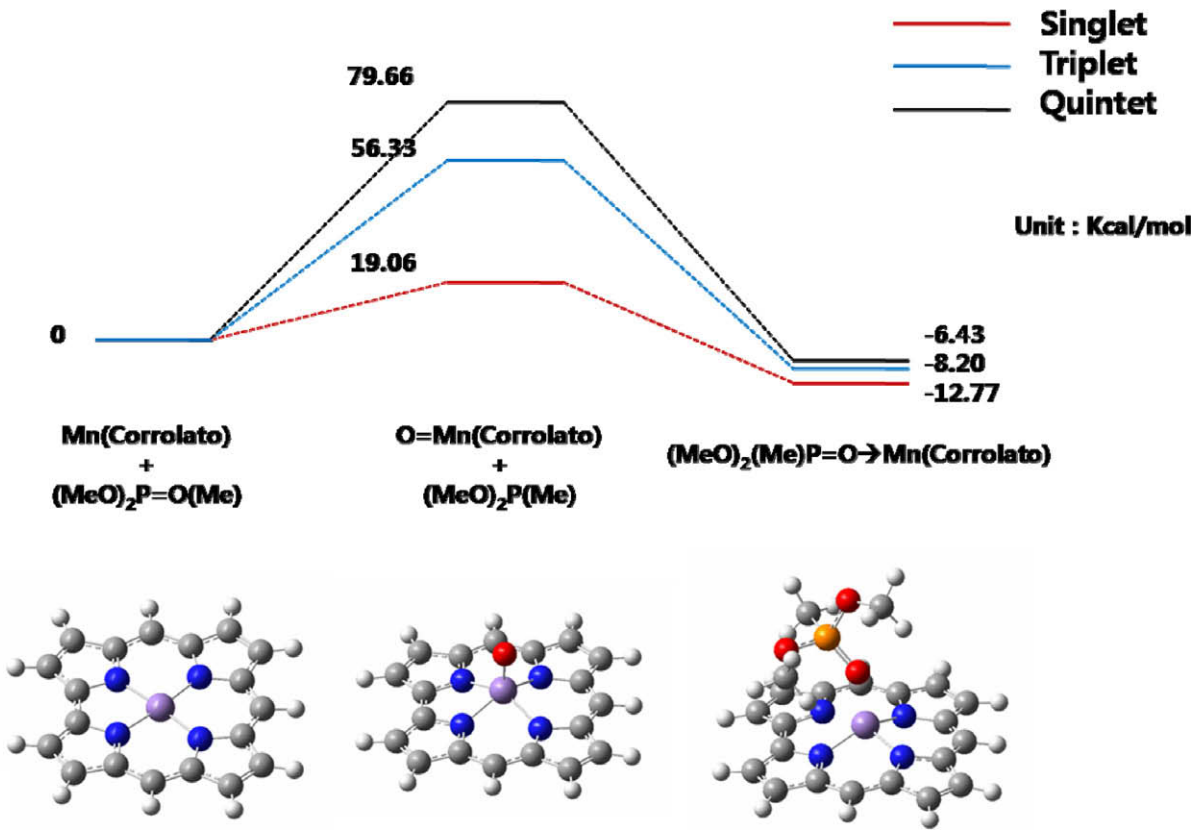

Fig. 11. Relative energies and geometries for three neutral manganese(III) corrolato species.

terminal oxo-derivative is evident, when compared to the corrolato counterpart. The oxo-intermediate is lowest for the doublet spin state; but the sextet actually "edges out" the doublet as the lowest energy species as the phosphonate adduct (right side set in Fig. 12). Clearly, the P═O will never oxidize the manganese in either the corrole or porphyrin case; and this obviously drives phosphine oxidation catalysis; how phosph*onites* might oxidize or *de*-oxidize in the context of nerve agent sensing and remediation is "food for thought." These calculations help in approaching or understanding the opportunities, and limitations of catalytic decontamination of organophosphonate-based chemical warefare agents. Structurally, the Mn–O–P angle in the Mn(pfp)corrolato is 158.6° and the metal exists 0.29 Å above the [N_4] mean plane [19a], the calculated Mn–O–P angles and manganese atom "out-of-plane" distances in these model systems depend on the spin state and are provided in Table 2 comparison for both the corrole and porphyrin adducts.

3. Conclusion

In this report we have described the preparation, characterization, and dynamics of new A_2B-corrole, *trans*-A_2B_2-porphyrin, and their manganese complexes. To our knowledge, this is the first

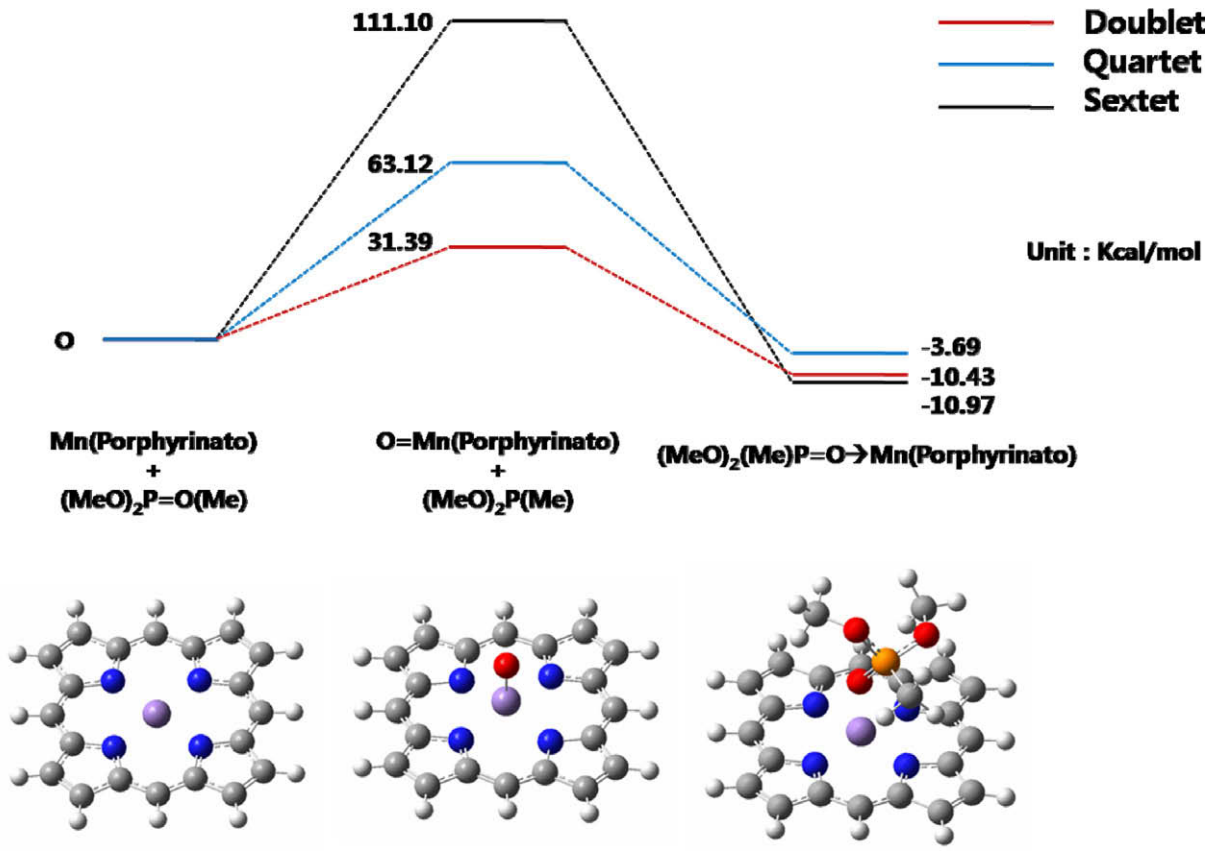

Fig. 12. Relative energies and geometries for three neutral manganese(II) porphyrinato species.

Table 2
Geometrical features in the calculated structures of Mn-porphyrinato and -corrolato species.

Mn-corrole multiplicity	Distance of Mn and [N_4] mean plane	Mn-corrole multiplicity	Mn–O–P angle
Singlet	0.54 Å	singlet	141.1°
Triplet	0.47 Å	triplet	136.3°
Quintet	0.36 Å	quintet	140.6°
Mn-porphyrin multiplicity		Mn-porphyrin multiplicity	
Doublet	0.29 Å	doublet	139.8°
Quartet	0.38 Å	quartet	141.1°
Sextet	0.11 Å	sextet	139.8°

determination of OP sensing capabilities of metallocorroles and metalloporphyrins. Also this is the first report of a *meso* 3-vinylphenyl substituted polypyrrole species. The synthesis for the metallocorroles and metalloporphyrin species is adapted from the literature. We undertook detailed NMR spectral characterization and obtained the structure of the free-base corrole (**1**) through the use of single-crystal X-ray diffraction. We probed the possibility of selective sensing of nerve agent model organophosphonate species. The bonding of organophosphonate to the Mn^{n+} center is supported by the strong responses in the UV–Vis spectrum upon analyte titration. This technique gave quantification of 1:1 binding for the Mn(PFP-VC)corrole (**3**) (PFP-VC = 5,15-di(pentafluorophenyl)-10-(3-vinylphenyl)corrolate) with $(CH_3CH_2O)_2P{=}O(C_3H_6NMe_2)$, $(C_4H_9O)_2P{=}O(Me)$, $(C_2H_5O)_2P{=}O(Me)$, and $(CH_3COCH_2)P{=}O(OC_2H_5)_2$. The titrimetric data allows for the calculated K_a values in the case of the [Mn(PFP-VP)][Cl] which ranged from 6.7 to 11.9 M^{-1}. These studies confirm 1:1 binding through the use of Job plots for compound **4** as well. Cyclic voltammetry of compounds was acquired for **1**-**4**; the values of the Mn(PFP-VC)corrole can be compared to those for Mn(Mes_2Ph)corrolato that appear in a recent report from Kadish and coworkers [25f]. Modeling of $O{=}P(OMe)_2Me$ binding and formal M–O or P–O cleavage products in bare neutral Mn-corrole and -porphyrins with different metal-based spin states was undertaken. These efforts revealed the effect of $(MeO)_2P{=}O(Me)$ phosphoryl O-atom binding using three different metal-based spin states. Regarding the minimum bare corrole/porphyrin organophosphonate binding energies, greater stability occurred for the Mn-corrole (singlet) and the Mn-porphyrin (sextet) than for other spin states studied. From this data, we can support that the corrole is a more sensitive platform for organophosphonate sensing and has a possibility to optically detect organophosphonate on at least the *micro*molar level because of clear changes that occur in the UV–Vis spectrum. This sensitivity is probably inadequate for current nerve agent applications as a stand-alone method, however. But it is hoped that this report will enable various further studies, especially in realm of nanoscience, and with respect to piezoelectric studies in which the response involves acoustic signals of mass differences, not optical signals. Also, these compounds can be studied in the presence of a variety of decomposition products (CN^-, F^-, phosphonic acids) that could be present under real "battlefield" conditions. Future studies, may include catalysis with these species [20b]; also an expansion

of this same analyte binding can be made to the related manganese-corrolazines.

4. Experimental

4.1. General considerations

All reagents and solvents herein were of analytical grade and used as received from reliable commercial sources. The reagents 3-vinylbenzaldehyde, DMF, TFA, DDQ, $F_3B{\cdot}OEt_2$, $Mn(OAc)_2{\cdot}4H_2O$ were purchased from Aldrich, USA; pentafluorophenylcarboxaldehyde was acquired from TCI, Japan; toluene, dichloromethane, and chloroform were acquired from Merck [30]. Dipyrromethane was prepared by literature report [22]. The synthetic procedures for A_2B corroles and their metallocorroles were adapted from the literature [23]. All solvents used for NMR spectral analysis were purchased commercially and were of spectroscopic grade. ^{1}H NMR spectra were measured in $CDCl_3$ or CD_2Cl_2 with Bruker Avance 300 and 400 MHz spectrometers. Spectral signals were calibrated by the *protio* impurity of the deuterated solvent. Infrared spectra were recorded with a Bruker Equinox 55 spectrophotometer; UV–Vis spectra were obtained with a JASCO V-503 UV–Vis spectrometer. A Vario EL III CHNS elemental analyzer was used in obtaining microanalysis values. High resolution MALDI mass spectrometry was performed by the staff of the research supporting team at KAIST on a VG AUTOSPEC ULTIMA with a trisector double focusing magnetic sector analyzer at a resolution of 80 000.

4.2. Preparation of 5,15-bis(pentafluorophenyl)-10-(3-vinylphenyl) corrole [H_3(PFP-VC)], (**1**)

A mixture of 5-(pentafluorophenyl)dipyrromethane (5.13 g, 16.4 mmol) and 3-vinylbenzaldehyde (1.04 mL, 8.2 mmol) and a dichloromethane solution of TFA (80 μL), were dissolved in 800 mL dichloromethane. The reaction mixture was stirred for 12 h. DDQ (4.47 g, 19.6 mmol) in toluene was added dropwise over several minutes accompanied by vigorous stirring, which continued for 15 additional minutes. The volume of the reaction mixture was then reduced and the mixture was filtered through a pad of silica (silica gel, CH_2Cl_2:hexane = 1:1), followed by column chromatography (silica gel, CH_2Cl_2:hexane 1:4) which ultimately gave a dark green solid. This compound was further purified by preparative TLC to give pure corrole, H_3(PFP-VC) (613 mg, 10.2%). MALDI-TOF: m/z $[M+H]^+$: 733.137 (calc); 733.791 (obs). ^{1}H NMR(δ, CD_2Cl_2): 9.15 (d, J_{H-H} = 4.17 Hz, $2H_{3,18}$), 8.76 (m, $4H_{8,9,12,13}$), 8.62 (d, J_{H-H} = 3.98 Hz, $2H_{4,17}$), 8.26 (s, $1H_f$), 8.09 (d, J_{H-H} = 7.22 Hz, $1H_j$), 7.83 (d, J_{H-H} = 7.86 Hz, $1H_h$), 7.74 (t, J_{H-H} = 7.58 Hz, $1H_i$), 7.00 (dd, J_{H-H} = 17.60, 10.94, $1H_k$), 5.97 (d, J_{H-H} = 17.56, $1H_{l\text{-}trans}$), 5.40 (d, J_{C-H} = 10.98, $1H_{l\text{-}cis}$). ^{13}C-NMR: 147.87, 145.42, 143.49, 141.96, 141.52, 140.96, 140.37, 139.66, 137.19 (t, $^1J_{C-H}$ = 82.6 Hz, C_k), 135.88, 134.54 (d, $^1J_{C-H}$ = 159.9 Hz, C_j), 132.93 (d, $^1J_{C-H}$ = 164.3 Hz, C_f), 132.01, 128.11 (d, $^1J_{C-H}$ = 173.2 Hz, $C_{8,13}$), 127.91 (d, $^1J_{C-H}$ = 159.5, C_i), 125.97 (d, $^1J_{C-H}$ = 147.6 Hz, C_h), 125.81 (d, $^1J_{C-H}$ = 172.0 Hz, $C_{9,12}$), 122.02 (d, ^1J = 170.1 Hz, $C_{4,17}$), 118.06 (dd, ^1J = 173.1 Hz, 3.5 Hz, $C_{3,18}$), 114.93 (dd, ^1J = 159.7 Hz, 6 Hz, C_l), 114.47, 113.543. ν_{N-H} (KBr): 3421 cm^{-1}.

4.3. Preparation of 5,15-bis(pentafluorophenyl)-10,20-bis(3-vinylphenyl)porphyrin [H_2(PFP-VP)] (**2**)

5-(Pentafluorophenyl)dipyrromethane (0.50 g, 1.6 mmol) and 3-(vinylphenyl)benzaldehyde (0.20 mL, 1.6 mmol) were added to a portion of chloroform (160 mL); $BF_3{\cdot}OEt_2$ (65 μL) was then added dropwise to this reaction mixture. The reaction mixture was stirred for 1 h at RT; DDQ (0.27 g, 1.2 mmol) in toluene was then added slowly. After 1 h, the reaction mixture was filtered through a silica gel pad followed by purification via silica gel column chromatography (CH_2Cl_2: hexane = 1: 1) which gave a purple solution. This solution was then evaporated to give a purple solid (247 mg, 37.2%). ^{1}H NMR ($CDCl_3$): δ 8.97 (d, J_{H-H} = 4.8 Hz, $H_{3,9,13,19}$), 8.80 (d, J_{H-H} = 4.8 Hz, $H_{4,8,14,18}$), 8.26 (s, $2H_f$), 8.11 (d, J_{H-H} = 7.5 Hz, $2H_j$), 7.86 (d, J_{H-H} = 7.9 Hz, $2H_h$), 7.73 (t, J_{H-H} = 7.6, $2H_i$), 6.99 (dd, J_{H-H} = 17.6, 10.9 Hz, $2H_k$), 5.96 (d, J_{H-H} = 17.5, $2H_{l\text{-}trans}$), 5.42 (d, J_{H-H} = 11.0, $2H_{l\text{-}cis}$), −2.82 (s, $2H_{N-H}$). MALDI-TOF: m/z $[M+H^+]$ 847.184 (calc); 847.666 (obs). ν_{N-H} (KBr): 3321 cm^{-1}. *Anal.* Calc. for $C_{48}H_{24}N_4F_{10}$: C, 68.09; H, 2.86; N, 6.62. Found: C, 66.99; H, 2.91; N, 6.46%.

4.4. Preparation of 5,15-bis(pentafluorophenyl)-10-(3-vinylphenyl) corrolate manganese(III) [Mn(PFP-VC)] (**3**)

A small round-bottom flask was charged with 15 mL of dry DMF, H_3(PFP-VC) (0.05 g, 0.068 mmol), and $Mn(OAc)_2{\cdot}4H_2O$ (0.05 g, 0.20 mmol) and was heated to reflux for 20 minutes. The complete consumption of H_3(PFP-VC) was confirmed through the use of TLC assaying. The reaction mixture was then allowed to cool to room temperature after which time the solvent was removed under reduced pressure. The resulting residue was purified by silica gel column chromatography (1:1, hexane:ethyl acetate) to give pure Mn(PFP-VC). The yield was 50.0 mg (94%). MALDI-TOF: m/z (M^+): 784.052 (calc); 784.215 (obs). *Anal.* Calc. for $C_{39}H_{15}N_4F_{10}Mn$: C, 59.71; H, 1.93; N, 7.14. Found: C, 59.66; H, 3.04; N, 6.08%. λ_{max} (log ε/(M^{-1} cm^{-1})): 601 (3.56); 411 (4.60) [soret band]; 356 (4.47).

4.5. Preparation of 5,15-bis(pentafluorophenyl)-10,20-bis(3-vinylphenyl)porphyrinato manganese(III) [Mn(PFP-VP)] chloride (**4**)

H_2(PFP-VP) (85 mg, 0.1 mmol) and manganese acetate tetrahydrate (101 mg, 0.41 mmol) were dissolved in DMF (10 mL). The reaction mixture was refluxed for 1 h, and was then allowed to cool to room temperature. A TLC assay revealed no trace of free-base porphyrin. The reaction mixture was then placed into a NaCl aqueous solution containing a portion of ice, which allowed a green precipitate to form. This solid was isolated by filtration and dried affording a (green) solid formulated as the mono-chloride **4** (85.1 mg, 91.1%). MALDI-TOF: m/z ($M-Cl^+$) 899.107 (calc), 899.427 (obs). λ_{max} (log ε/(M^{-1} cm^{-1})): 609 (3.68); 576 (3.88); 475 (4.90) [Soret band]; 396 (4.52); 369 (4.67).

4.6. X-ray structural determination of compound **1**

A single crystal of **1** was mounted on a goniometer and data were collected on a Bruker P4 diffractometer equipped with a SMART CCD detector using graphite-monochromated Mo Kα radiation (λ = 0.71073 Å). The structure was solved using direct methods and standard difference map techniques, and was refined by full-matrix least-squares procedures on F^2 with SHELXTL (version 5.10). Cell parameters were determined and refined by the SMART program [31a]. Data reduction was performed by using SAINT software [31a]. The data were corrected for Lorentz and polarization effects. An empirical absorption correction was applied using the SADABS program [31b]. The structures were solved by direct methods using the program SHELXS-97 [31c] and refined by full matrix least-squares calculations (F2) by using the SHELXL-97 software [31d]. All non-H atoms were refined anisotropically against F^2 for all reflections. All hydrogen atoms were placed at their calculated positions and refined isotropically. Crystal data, data collection and refinement parameters are summarized in the caption of Fig. 10.

4.7. Modeling of analyte binding

For non-linear fitting, we have used Eq. (1) [32,33] to determine 1:1 stoichiometry in our Mn-corrole and Mn- porphyrin systems.

$$A = A_0 + \frac{A_{\lim} - A_0}{2c_0}\left[c_0 + c_M + \frac{1}{K_s} - \left[\left(c_0 + c_M + \frac{1}{K_s}\right)^2 - 4c_0c_M\right]^{1/2}\right] \quad (1)$$

The parameters are as follows: A = absorbance, C_0 = concentration of corrole or porphyrin; K_s = binding constant, C_M = concentration of organophosphonate analyte, A_0 = absorbance of corrole or porphyrin; A_{lim} = absorbance when analyte is bound completely.

4.8. Cyclic voltammetry (CV)

Measurements were carried out with a BAS 100B instrument (Bioanalytical Systems, Inc). A three-electrode system was used consisting of a gold disk working electrode, a platinum wire counter electrode, and an Ag/Ag^+ electrode (MF-2062 kit, Bioanalytical Systems, Inc.) as the reference electrode. The Ag/Ag^+ contained 0.1 M tetrabutylammonium perchlorate (TBAP) and 0.01 M $AgNO_3$ in benzonitrile. In 0.1 M TBAP, the $E_{1/2}$ of the ferrocene/ferrocenium ion couple was taken to be 0.067 V versus Ag/Ag^+ in benzonitrile. The values in electrochemical experiments are reported versus the ferrocene/ferrocenium ion [29] redox couple.

4.9. Computational details

The GAUSSIAN 03 program was used for all calculational work [34]. All geometries were processed *in silico* in the gas phase at 0 K. The following protocol was used for all calculations: (i) input geometries were derived from the crystallographic structures provided herein where possible, or by careful modification of closely related geometries and invoking chemical intuition. (ii) Density functional theory (DFT) geometry optimizations were performed using B3LYP hybrid functional with the LACVP* (double zeta) basis set. The basis set used the Lanl2DZ effective core potential (ECP) for the manganese atom, and 6-31G(d) for all other atoms.

Acknowledgements

D.G.C. acknowledges support from the Korea Science and Engineering Foundation (KOSEF) Grant (No. R01-2008-000-12388-0), funded by the Korean Government (MOST). Professor Y.S.L. and I.K. (Quantum Chemistry Laboratory) gratefully acknowledge (i) financial support from the Korea Science and Engineering Foundation (Nos. R01-2007-000-11015-0, R11-2007-012-03001-0) and (ii) computational time from the supercomputing center of KISTI. Professor Gerard Parkin (Department of Chemistry, Columbia University) facilitated the X-ray diffraction study of Compound **1**. MALDI-TOF analyses were obtained with the help of the KAIST research supporting team. Hack Soo Shin is gratefully acknowledged for his help in acquiring NMR data. Dr. Raj Chakrabarti (former NIH Postdoctoral fellow at the Departments of Chemistry at M.I.T. & Columbia University) is acknowledged for helpful discussions during his visit to KAIST (July, 2005). Teresa Lindstead (Cambridge, England) is thanked for her assistance in filing our crystallographic data (CCDC 684999).

Appendix A. Supplementary data

CCDC 684999 contains the supplementary crystallographic data for this paper. These data can be obtained free of charge via www.ccdc.cam.ac.uk/conts/retrieving.html, or from the Cambridge Crystallographic Data Centre, 12 Union Road, Cambridge CB2 1EZ, UK; fax: (+44) 1223-336-033; or e-mail: deposit@ccdc.cam.ac.uk.

Supplementary data associated with this article can be found, in the online version, at doi:10.1016/j.poly.2009.04.020.

References

[1] B. Meunier, Heme-peroxidases, in: J.A. McCleverty, T.J. Meyer (Eds.), Comprehensive Chemistry II, vol. 8, 2004, p. 261.
[2] I. Aviv, Z. Gross, Chem. Commun. (2007) 1987.
[3] D.T. Gryko, B. Koszarna, Org. Biomol. Chem. 1 (2003) 350.
[4] D.T. Gryko, Chem. Commun. (2000) 2243.
[5] E. VanCaemelbecke, S. Will, M. Autret, V.A. Adamian, J. Lex, J.P. Gisselbrecht, M. Gross, E. Vogel, K.M. Kadish, Inorg. Chem. 35 (1996) 184.
[6] M. Autret, S. Will, E. Vancaemelbecke, J. Lex, J.P. Gisselbrecht, M. Gross, E. Vogel, K.M. Kadish, J. Am. Chem. Soc. 116 (1994) 9141.
[7] (a) S. Nardis, D. Monti, R. Paolesse, Mini-Rev. Org. Chem. 2 (2005) 355;
(b) S. Nardis, F. Mandoj, R. Paolesse, F.R. Fronczek, K.M. Smith, L. Prodi, M. Montalti, G. Battistini, Eur. J. Inorg. Chem. (2007) 2345.
[8] G. Parkin, J. Chem. Educ. 83 (5) (2006) 791.
[9] J.-M. Barbe, G. Canard, S. Brandes, F. Jerome, G. Dubois, R. Guilard, Dalton Trans. (2004) 1208.
[10] R. Czolk, Sens. Actuators B B30 (1996) 61.
[11] R. Paolesse, C. Di Natale, A. Macagnano, F. Sagene, M.A. Scarselli, P. Chiaradia, V.I. Troitsky, T.S. Berzina, A. D'Amino, Langmuir 15 (1999) 1268–1274.
[12] C. Di Natale, C. Goletti, R. Paolesse, M. Drago, A. Macagnano, A. Mantini, V.I. Troitsky, T.S. Berzina, M. Cocco, A. D'Amico, Sens. Actuators B B57 (1999) 183.
[13] A. D'Amico, C. Di Natale, A. Macagnano, F. Davide, A. Mantini, E. Tarizzo, R. Paolesse, T. Boschi, Biosens. Bioelectron. 13 (1998) 711.
[14] (a) T.A. Romanova, O.V. Kravchenko, I.I. Morgulis, A.A. Kuzubov, P.O. Krasnov, P.V. Avramov, Koord. Khim. 30 (2004) 403;
(b) S. Han, K. Cho, J. Ihm, Phys. Rev. E: Stat. Phys., Plasmas, Fluids 19 (1999) 2218.
[15] R. Zwaans, J.H. van Lenthe, D.H.W. den Boer, Theochem 339 (1995) 153.
[16] J.W. Grate, S.N. Kaganove, Strongly Hydrogen-Bond Acidic Polymer and Methods of Making and Using, US Patent 6015,869, January 2000.
[17] D.A. Atwood, D.G. Churchill, "Destruction and detection of chemical warfare agents", Chem. Rev., cr-2008-00223w, in preparation.
[18] Z. Gross, G. Golubkov, L. Simkhovich, Angew. Chem., Int. Ed. 39 (2000) 4045.
[19] (a) J. Bendix, H.B. Gray, G. Golubkov, Z. Gross, Chem. Commun. (2000) 1957;
(b) The report by D.P. Goldberg on corrolazines is particulary relevant to the discussion herein:B.S. Mandimutsira, B. Ramdhanie, R.C. Todd, H. Wang, A.A. Zareba, R.S. Czernuszewicz, D.P. Goldberg, J. Am. Chem. Soc. 124 (2002) 15170;
(c) S. Licoccia, E. Morgante, R. Paolesse, F. Polizio, M.O. Senge, E. Tondello, T. Boschi, Inorg. Chem. 36 (1997) 1564.
[20] (a) Preliminary presentations of portions of this work include two poster presenations: K. Kim, N. Maiti, D.G. Churchill, Abstracts of Papers, 235th ACS National Meeting, New Orleans, LA, United States, April 6–10, 2008, INOR-192.;
(b) K. Kim, N. Maiti, D.G. Churchill, Abstracts of Papers, 234th ACS National Meeting, Boston, MA, United States, August 19–23, 2007, INOR-660.;
(c) D.G. Churchill, N. Maiti, S.H. Choi, Metallocorrole catalyst produced by substituting 3-vinyl phenyl group from a corrole compound and a method for producing the same, Repub. Korean Kongkae Taeho Kongbo (2007), CODEN: KRXXA7 KR 2007049466 A 20070511 CAN 147:475473 AN 2007:1191159 (Note, the first two authors were erroneously listed as David, G.C. and Nilkamal, M.).;
(d) Oxygen-atom transfer catalysis has previously been explored with Compound **3**: N. Maiti, K. Kim, B. Meka, D.G. Churchill, unpublished results, 2005–2007.
[21] D.L. Pilloud, C.C. Moser, K.S. Reddy, P.L. Dutton, Langmuir 14 (1998) 4809.
[22] B.J. Littler, M.A. Miller, C.H. Hung, R.W. Wagner, D.F. O'Shea, P.D. Boyle, J.S. Lindsey, J. Org. Chem. 64 (1999) 1391.
[23] D.T. Gryko, B. Koszarna, Synthesis (2004) 2205.
[24] (a) N. Maiti, J. Lee, Y. Do, H.S. Shin, D.G. Churchill, J. Chem. Crystallogr. 35 (2005) 949;
(b) N. Maiti, J. Lee, S.J. Kwon, J. Kwak, Y. Do, D.G. Churchill, Polyhedron 25 (2006) 1519.
[25] [a] The isolation of the porphyrin from the corrole reaction involves preparative TLC. This however would favor migration of Mn(II) which is not ionic; as the Mn(II) migrates on silica in air, it may decompose and become the oxo (manganyl) species (ligand oxidation may also occur). The Mn(II) species however, is less stable than the [Mn(III)Cl] porphyrin species which can be more completely synthesized as chloride salt as discussed herein and reported previously.;
(b) R.D. Jones, D.A. Summerville, F. Basolo, J. Am. Chem. Soc. 100 (1978) 4416;
(c) While the formulation of the porphyrin is Mn(III), it is well known that upon appropriate oxidant, the preparation can be made for Mn(IV) (e.g., using ^{t}BuOOH) and Mn(V) (e.g., using H_2O_2):W. Nam, I. Kim, M.H. Lim, H.J. Choi, J.S. Lee, H.G. Jang, Chem. Eur. J. 8 (2002) 2067;
(d) D. Turner, M.J. Gunter, Inorg. Chem. 33 (1994) 1406;
(e) Z. Ou, C. Erben, M. Autret, S. Will, D. Rosen, J. Lex, E. Vogel, K.M. Kadish, J. Porphyrins Phthalocyanines 9 (2005) 398;

(f) J. Shen, M.E. Ojaimi, M. Chkounda, C.P. Gros, J.-M. Barbe, J. Shao, R. Guilard, K.M. Kadish, Inorg. Chem. 47 (2008) 7717. See references herein for previous electrochemical studies of a variety of Mn corroles, e.g., octaethyl substituted corrole-based systems.

[26] I. Bandyopadhyay, M.J. Kim, Y.S. Lee, D.G. Churchill, J. Phys. Chem. A 110 (2006) 3655.

[27] It is thought that a carefully positioned carboxylic acid or related group could effect secondary *N*-binding of this analyte in the context of selective VX binding.

[28] (a) G. Golubkov, J. Bendix, H.B. Gray, A. Mahammed, I. Goldberg, A.J. DiBilio, Z. Gross, Angew. Chem., Int. Ed. 40 (2001) 2132;
[b] An Mn(III) porphyrinato would require the use of an anion for electroneutrality; this was not pursued in these calculations. The point of this work was to seek an understanding of the diversity of the various spin states, which was done through the analysis of neutral systems. A Mn(III)porphyrinato species would be more electron deficient at the metal center (on average) and this would be expected to *strengthen* the organophosphonate dative interaction.

[29] (a) M.K. Tse, Z. Zhang, K.S. Chan, Chem. Commun. (1998) 1199;
(b) A.E. Meier-Callahan, H.B. Gray, Z. Gross, Inorg. Chem. 39 (2000) 3605;
(c) H.-Y. Chao, D.G. Churchill, J. Chem. Educ. 85 (2008) 1210;
(d) O.A. Egorova, O.G. Tsay, S. Khatua, J.O. Huh, D.G. Churchill, Inorg. Chem, in press.

[30] With regards to laboratory safety, a useful description of some common laboratory chemical explosion hazards has been prepared: D.G. Churchill, J. Chem. Educ. 83 (2006) 1798.

[31] [a] SMART and SAINT, Area Detector Software Package and SAX Area Detector Integration Program; Bruker Analytical X-ray, Madison, WI, 1997.;
[b] SADABS, Area Detector Absorption Correction Program; Bruker Analytical X-ray: Madison, WI, 1997.;
[c] G.M. Sheldrick, SHELXS-97 program for crystal structure determination, Acta Crystallogr. A46 (1990) 467–473.;
[d] G. Sheldrick, SHELXL-97, Universität Göttingen, Göttingen, Germany, 1999.

[32] B. Valeur, J. Pouget, J. Bourson, M. Kaschke, N.P. Ernsting, J. Phys. Chem. 96 (1992) 6545.

[33] ORIGIN 6.1, Windows-Based Scientific Graphing and Data Analysis Software, OriginLab Co. Northampton, MA, USA.

[34] GAUSSIAN 03: M.J. Frisch et al., Gaussian Inc., Wallingford CT, 2004 (see Supplementary Supporting Information for complete citation).